[2]Ifju, P., Jenkins, D., Ettinger, S., Lian, Y., Shyy, W., and Waszak, R. M., "Flexible-Wing-Based Micro Air Vehicles," AIAA Paper 2002-0705, Jan. 2002.

[3]Oden, J. T., and Sato, T., "Finite Strains and Displacements of Elastic Membranes by the Finite Element Method," *International Journal of Solids and Structures*, Vol. 3, 1967, pp. 471–488.

[4]Green, A. E., and Adkins, J. E., *Large Elastic Deformations*, Clarendon, Oxford, 1960.

[5]Jackson, P. S., and Christie, G. W., "Numerical Analysis of Three-Dimensional Elastic Membrane Wings," *AIAA Journal*, Vol. 25, 1987, pp. 676–682.

[6]Smith, R. W., and Shyy, W., "A Viscous Flow Based Membrane Wing Model," AIAA Paper 93-2955, July 1993.

[7]Shyy, W., and Smith, R. W., "Computation of Laminar Flow and Flexible Structure Interaction," *Computational Fluid Dynamics Review*, edited by M. Hafez and K. Oshima, Wiley, Chichester, England, U.K., 1995, pp. 777–796.

[8]Lian, Y., Shyy, W., Ifju, P., and Verron, E., "A Computational Model for Coupled Membrane-Fluid Dynamics," AIAA Paper 2002-2972, June 2002.

[9]Shyy, W., *Computational Modeling for Fluid Flow and Interfacial Transport*, Elsevier, Amsterdam, 1994, revised printing 1997.

[10]Mooney, M., "A Theory of Large Elastic Deformation," *Journal of Applied Physics*, Vol. 11, 1940, pp. 582–592.

[11]Lian, Y., Steen, J., Trygg-Wilander, M., and Shyy, W., "Low Reynolds Number Turbulent Flows Around a Dynamically Shaped Airfoil," *Computers and Fluids*, Vol. 32, March 2003, pp. 287–303.

[12]Duchon, J. P., "Splines Minimizing Rotation-Invariant Semi-Norms in Sobolev Spaces," *Constructive Theory of Functions of Several Variables*, edited by W. Schempp and K. Zeller, Springer, Berlin, 1977, pp. 85–100.

A. Plotkin
Associate Editor

Enhancement of Damage Identification Through Structural Matrix Assignment

Jason A. Solbeck* and Laura R. Ray†
Dartmouth College,
Hanover, New Hampshire 03755-8000

I. Introduction

SENSING damage in structures through vibration data is hindered by lack of sensitivity of measurable quantities, such as natural frequency and mode shapes, and identifiable quantities, such as mass and stiffness parameters, to damage. Sensitivity enhancing control (SEC) exploits the relationship between feedback control gains and system behavior to enhance changes in vibration characteristics when damage occurs. The ultimate goal of SEC is to aid in damage detection and localization in smart structures through this enhanced sensitivity. Ray and Tian[1] investigate full-state feedback control laws for sensitivity enhancement of the change in natural frequency caused by stiffness damage through simulation of a cantilevered beam in bending. Ray et al.[2] investigate the ability to enhance the sensitivity of frequency shifts as a result of fatigue cracks in a plate. These papers provide evidence that SEC enhances sensitivity to stiffness damage significantly. However, in both studies feedback control laws were designed based on analytic models of the structure, which in practice, might not be available or might contain error, and both studies incorporate full-state feedback. Ideally, a healthy model would be identified entirely from input and output data from the structure under investigation. This model would then be used to develop a sensitivity-enhancing controller for diagnosing the presence or absence of future structural damage from available measurements.

The problem of implementing SEC for a system without an analytic model was approached by Solbeck et al.[3] That study shows that a primary issue in damage identification using the SEC methodology is that of identifying a healthy model from the input and output data in physical coordinates, such that damage-induced mass, stiffness, and damping changes ultimately can be identified. The present study addresses this problem. A robust implementation of observer-Kalman filter identification (OKID)[4] is used to identify an initial minimum-order model for the healthy system. This model is then transformed using common basis-normalized structural identification (CBSI)[5] into a form from which the mass, damping, and stiffness matrices can be identified, provided that there are as many measurements as degrees of freedom.

Given an identified or analytic model, identifying damage from measured modal frequencies and mode shapes takes the form of either a forward or inverse problem. The forward problem uses an identified or analytic model to predict the effect of hypothesized damage cases (e.g., location and/or damage magnitude) on modal frequencies, which are then compared with measured modal frequencies to determine the most likely damage case. The inverse problem uses optimization to update structural stiffness, mass, and/or damping matrices based on measured modal properties to minimize the difference between measured and model-predicted modal properties. For either method success depends heavily on the number of measured modal frequencies and/or mode shapes. To improve damage identification algorithms, methods have been developed for modifying the structure to enhance the information set that is used with forward or inverse approaches. Nalitolela et al.[6] used the concept of adding known physical masses or stiffnesses to a system to provide additional modal frequencies for model updating from modal frequencies alone. Cha and Gu[7] used the same concept, along with a model updating formulation that enforces known connectivity between structural elements. Lew and Juang[8] introduced the concept of using feedback controllers to mimic the addition of masses and stiffnesses to a system.

In this Note a structural matrix assignment (SMA) method is developed in which a controller directly changes, or "assigns," the effective stiffness and damping matrices of a feedback controlled structure. By shifting the effective (closed-loop) stiffness matrix to a smaller value, changes in stiffness caused by damage become more easily identifiable. SMA avoids reliance on measured modal frequencies and mode shapes for identifying damage. Instead, the elements of a closed-loop stiffness matrix are identified directly. The OKID and CBSI methods are used for identification, whereas concepts from Refs. 1 and 2 are used to target a closed-loop stiffness matrix to be assigned. The SMA method is developed in Sec. II.C and applied to a three-degree-of-freedom system subject to stiffness damage in Sec. III.

II. Theory

A. Structural Dynamics

The second-order, linear equation of motion for a dynamic structure with m degrees of freedom, r inputs, and q outputs is given by

$$\mathcal{M}\ddot{\boldsymbol{z}} + \mathcal{D}\dot{\boldsymbol{z}} + \mathcal{K}\boldsymbol{z} = \mathcal{B}\boldsymbol{u} \tag{1}$$

$$\boldsymbol{y} = \boldsymbol{H}_d\boldsymbol{z} + \boldsymbol{H}_v\dot{\boldsymbol{z}} + \boldsymbol{H}_a\ddot{\boldsymbol{z}} \tag{2}$$

$\mathcal{M}$, $\mathcal{D}$, and $\mathcal{K}$, are the $m \times m$ mass, damping, and stiffness matrices; $\boldsymbol{H}_d$, $\boldsymbol{H}_v$, and $\boldsymbol{H}_a$ are the $q \times m$ displacement, velocity, and acceleration output influence matrices; $\mathcal{B}$ is the $m \times r$ input influence matrix; and $\boldsymbol{z}$, $\boldsymbol{u}$, and $\boldsymbol{y}$ are the $m \times 1$ position vector, the $r \times 1$ input force vector, and the $q \times 1$ output vector.

Received 24 February 2003; revision received 15 August 2003; accepted for publication 20 August 2003.

*Ph.D. Candidate, Thayer School of Engineering, 8000 Cummings Hall. Student Member AIAA.

†Associate Professor, Thayer School of Engineering, 8000 Cummings Hall.

For the case of proportional damping the damping matrix is expressed as a linear combination of $\mathcal{M}$ and $\mathcal{K}$:

$$\mathcal{D} = \alpha\mathcal{M} + \beta\mathcal{K} \tag{3}$$

Equation (1) is mass normalized by a change of basis using the eigenvectors of the generalized undamped eigenproblem:

$$\mathcal{K}\boldsymbol{\Phi} = \mathcal{M}\boldsymbol{\Phi}\boldsymbol{\Omega} \tag{4}$$

The new basis is defined such that $q = \boldsymbol{\Phi}\boldsymbol{\eta}$, resulting in a new equation of motion:

$$\ddot{\boldsymbol{\eta}} + \boldsymbol{\Xi}\dot{\boldsymbol{\eta}} + \boldsymbol{\Omega}\boldsymbol{\eta} = \boldsymbol{\Phi}^T\mathcal{B}\boldsymbol{u} \tag{5}$$

$$\boldsymbol{y} = \boldsymbol{H}_d\boldsymbol{\Phi}\boldsymbol{\eta} + \boldsymbol{H}_v\boldsymbol{\Phi}\dot{\boldsymbol{\eta}} + \boldsymbol{H}_a\boldsymbol{\Phi}\ddot{\boldsymbol{\eta}} \tag{6}$$

where

$$\boldsymbol{\Phi}^T\mathcal{M}\boldsymbol{\Phi} = \boldsymbol{I}_{m\times m} \tag{7}$$

$$\boldsymbol{\Phi}^T\mathcal{D}\boldsymbol{\Phi} = \boldsymbol{\Xi} \tag{8}$$

$$\boldsymbol{\Phi}^T\mathcal{K}\boldsymbol{\Phi} = \boldsymbol{\Omega} = \operatorname{diag}\left\{\omega_{ni}^2,\ i = 1, \ldots, m\right\} \tag{9}$$

Next, the state vector $\boldsymbol{x}$ with $n = 2m$ elements is defined as the set of modal positions and modal velocities of the system at discrete degrees of freedom along the structure:

$$\boldsymbol{x} = \begin{bmatrix}\boldsymbol{\eta}\\ \dot{\boldsymbol{\eta}}\end{bmatrix} \tag{10}$$

This allows Eqs. (5) and (6) to be rewritten in state-space form:

$$\dot{\boldsymbol{x}} = \begin{bmatrix}\boldsymbol{0}_m & \boldsymbol{I}_m\\ -\boldsymbol{\Omega} & -\boldsymbol{\Xi}\end{bmatrix}\boldsymbol{x} + \begin{bmatrix}\boldsymbol{0}_{m\times r}\\ \boldsymbol{\Phi}^T\mathcal{B}\end{bmatrix}\boldsymbol{u} \tag{11}$$

$$\boldsymbol{y} = [\boldsymbol{H}_d\boldsymbol{\Phi} - \boldsymbol{H}_a\boldsymbol{\Phi}\boldsymbol{\Omega} \quad \boldsymbol{H}_v\boldsymbol{\Phi} - \boldsymbol{H}_a\boldsymbol{\Phi}\boldsymbol{\Xi}]\boldsymbol{x} + \boldsymbol{H}_a\boldsymbol{\Phi}\boldsymbol{\Phi}^T\mathcal{B}\boldsymbol{u} \tag{12}$$

B. Structural Identification

In this study identification of mass, damping, and stiffness matrices is done in two steps. OKID[4] identifies a series of Markov parameters from the input and output data and extracts a realization of the first-order, state-space matrices, using the eigensystem realization algorithm.[9] To handle process and measurement noise, it is standard procedure to identify a model of much greater order than the expected true order of the model. The additional modes identified are known as noise modes. To separate the true structural modes from the noise modes, a second model of a different order is identified from the same input and output data. Only the eigenvalues of the structural modes will match between the two models, which allows the structural modes to be extracted from the higher-order identified model. This robust process allows minimum-order models to be identified reliably from noise-corrupted input and output data.

Second, using CBSI,[5] the state-space model is transformed into the form of Eqs. (11) and (12). From these equations the matrices $\boldsymbol{\Omega}$ and $\boldsymbol{\Xi}$ can be directly extracted. If there are at least as many outputs as degrees of freedom, then $\boldsymbol{\Phi}$ can be estimated allowing matrices $\mathcal{M}$, $\mathcal{D}$, and $\mathcal{K}$ to be estimated. The transformations of the CBSI algorithm are entirely deterministic for a given state-space realization. There is a problem when the model possesses nonproportional damping, which is often the situation when a model is identified from noise-corrupted data. In this case the modes are complex, and the estimates are somewhat corrupted, but this does not affect the following algorithm.

C. Structural Matrix Assignment

For output feedback with an $r \times 1$ external input vector $\boldsymbol{u}_c$ and an $r \times q$ feedback gain matrix $\boldsymbol{F}$, the system input is

$$\boldsymbol{u} = \boldsymbol{u}_c - \boldsymbol{F}\boldsymbol{y} \tag{13}$$

Combining Eq. (13) with Eqs. (1) and (2) yields an expression for the closed-loop system:

$$\mathcal{M}\ddot{\boldsymbol{z}} + \mathcal{D}\dot{\boldsymbol{z}} + \mathcal{K}\boldsymbol{z} = \mathcal{B}\boldsymbol{u}_c - \mathcal{B}\boldsymbol{F}\boldsymbol{H}_d\boldsymbol{z} - \mathcal{B}\boldsymbol{F}\boldsymbol{H}_v\dot{\boldsymbol{z}} - \mathcal{B}\boldsymbol{F}\boldsymbol{H}_a\ddot{\boldsymbol{z}} \tag{14}$$

or

$$(\mathcal{M} + \mathcal{B}\boldsymbol{F}\boldsymbol{H}_a)\ddot{\boldsymbol{z}} + (\mathcal{D} + \mathcal{B}\boldsymbol{F}\boldsymbol{H}_v)\dot{\boldsymbol{z}} + (\mathcal{K} + \mathcal{B}\boldsymbol{F}\boldsymbol{H}_d)\boldsymbol{z} = \mathcal{B}\boldsymbol{u}_c \tag{15}$$

By comparing Eq. (15) with Eq. (1), expressions for the effective closed-loop mass, damping, and stiffness are

$$\bar{\mathcal{M}} = \mathcal{M} + \mathcal{B}\boldsymbol{F}\boldsymbol{H}_a, \qquad \bar{\mathcal{D}} = \mathcal{D} + \mathcal{B}\boldsymbol{F}\boldsymbol{H}_v, \quad \text{and} \quad \bar{\mathcal{K}} = \mathcal{K} + \mathcal{B}\boldsymbol{F}\boldsymbol{H}_d \tag{16}$$

When the outputs are distinct displacements, velocities, and accelerations, $\boldsymbol{F}$ can be partitioned into a stiffness portion, a damping portion, and a mass portion. When there are q_1 position outputs, q_2 velocity outputs, and q_3 acceleration outputs ($q = q_1 + q_2 + q_3$), the expressions for $\boldsymbol{H}_d$, $\boldsymbol{H}_v$, and $\boldsymbol{H}_a$ can be rewritten

$$\boldsymbol{H}_d = \begin{bmatrix}\boldsymbol{H}_{d1}\\ \boldsymbol{0}_{q_2\times m}\\ \boldsymbol{0}_{q_3\times m}\end{bmatrix}, \qquad \boldsymbol{H}_v = \begin{bmatrix}\boldsymbol{0}_{q_1\times m}\\ \boldsymbol{H}_{v2}\\ \boldsymbol{0}_{q_3\times m}\end{bmatrix}, \qquad \boldsymbol{H}_a = \begin{bmatrix}\boldsymbol{0}_{q_1\times m}\\ \boldsymbol{0}_{q_2\times m}\\ \boldsymbol{H}_{a3}\end{bmatrix} \tag{17}$$

The feedback gain matrix is partitioned as $\boldsymbol{F} = [\boldsymbol{F}_1, \boldsymbol{F}_2, \boldsymbol{F}_3]$, and Eq. (16) becomes

$$\bar{\mathcal{M}} = \mathcal{M} + \mathcal{B}\boldsymbol{F}_3\boldsymbol{H}_{a3}, \qquad \bar{\mathcal{D}} = \mathcal{D} + \mathcal{B}\boldsymbol{F}_2\boldsymbol{H}_{v2}$$
$$\bar{\mathcal{K}} = \mathcal{K} + \mathcal{B}\boldsymbol{F}_1\boldsymbol{H}_{d1} \tag{18}$$

Clearly, the ability of the closed-loop system to recreate desired effective mass, damping, and stiffness depends heavily on the input and output influence matrices. In addition, to fully specify any effective structural matrix it is necessary that there be as many inputs as degrees of freedom and as many corresponding outputs as degrees of freedom, for example, displacement outputs for stiffness matrix specification. Otherwise, it is not possible to independently affect each element of the effective closed-loop structural matrix.

The design process for $\boldsymbol{F}$ is guided by the idea of improving sensitivity of the system response to changes in stiffness[1,2] by reducing the closed-loop effective stiffness, so that changes in stiffness caused by damage in the controlled structure are greater percent changes in total stiffness than for the open-loop system.

III. Simulation Methods and Results

Simulations were performed in MATLAB® using a three-degree-of-freedom spring-mass chain, in which three masses (each 1 kg) are connected in series via springs (each nominally 10 N/m), and the first mass is connected to ground. Normally distributed parameter variations with a standard deviation of 0.1 N/m are introduced into the stiffness of the springs, representing normal changes in structural parameters, for example, because of environmental conditions. Random process and measurement noise, each with a magnitude of 0.5%, are injected during initial excitation into the input and the output. Damping is initially proportional, with $\alpha = 0$ and $\beta = 0.05$, but because of identification issues described in Sec. II.B, the realized model typically exhibits nonproportional damping. A total of 10,000 data points are collected, sampling at 5 Hz.

The information used in subsequent calculations for stiffness damage identification are the uncorrupted input data, the noise-corrupted output data, the sampling interval, and knowledge of sensor and actuator locations. This ensures that the simulation is as realistic as possible.

A minimum-order state-space realization is determined using OKID as described earlier. This model is then transformed using

CBSI, so that the identified mass, stiffness, and damping matrices can be extracted. This process is repeated using a total of 20 input–output data sequences, and the identified structural matrices are averaged to remove the effects of parameter variation.

Using the average identified stiffness and damping matrices, a feedback gain was determined to provide the desired closed-loop effective stiffness, in this case roughly 5% of the open-loop stiffness. The feedback gain is then used to control a series of healthy and damaged models to compare the ability to discern damage in open- and closed-loop scenarios. To test for damage, the OKID-CBSI process is applied, and the diagonal elements of the identified stiffness matrices are examined.

In the first example full-state feedback is assumed to allow both the effective closed-loop stiffness and damping to be assigned. Because the full state is rarely available, in the second example, only position feedback is used, allowing the closed-loop effective stiffness to be assigned, but not the damping. In both examples the damage case is a 1% decrease in the stiffness of the third spring k_3, which reduces the second and third diagonal elements of the stiffness matrix, K_{22} and K_{33}.

To compare populations in the upcoming simulations, a hypothesis test is used. The null hypothesis is the means are equal, with the alternate hypothesis that the means differ. Because the variances of the two populations are unknown, but can be assumed to be equal, the test statistic is

$$T \equiv \frac{\bar{X}_1 - \bar{X}_2}{\sqrt{S_p^2(1/L_1 + 1/L_2)}} \tag{19}$$

where $\bar{X}_1$ and $\bar{X}_2$ are the population means, L_1 and L_2 are the population sizes, and

$$S_p^2 \equiv \frac{(L_1 - 1)S_1^2 + (L_2 - 1)S_2^2}{L_1 + L_2 - 2} \tag{20}$$

S_1^2 and S_2^2 are the population variances. Higher values of the test statistic T indicate a more significant difference in means between the two populations.

Figure 1 shows full-state feedback simulation results providing identified stiffness matrix diagonal elements for 20 trials. For both the healthy and damaged systems the variations in identified stiffness matrix diagonal elements are caused by both normal parameter variation and corruption in the input and output data used for identification. In the open-loop plots the effect of a 1% decrease in the stiffness of k_3 is only discernable in the third diagonal element of the

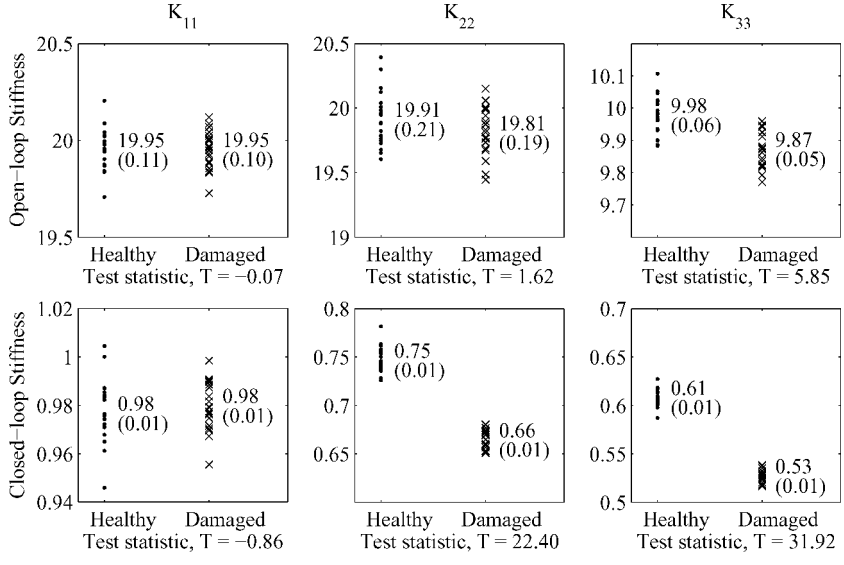

Fig. 1 Diagonal elements of the identified stiffness matrices in newtons/meter for the open-loop system and for the full-state feedback, closed-loop system. Mean value and standard deviation (in parentheses) are provided, and the test statistic is shown in the abscissa label.

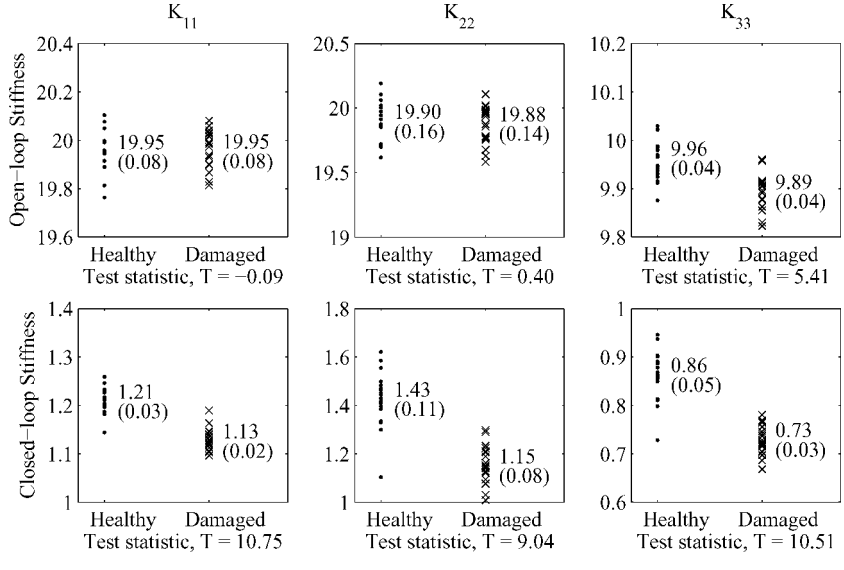

Fig. 2 Diagonal elements of the identified stiffness matrices in newtons/meter for the open-loop system and for the position feedback, closed-loop system. Mean value and standard deviation (in parentheses) are provided, and the test statistic is shown in the abscissa label.

stiffness matrix, and this shift would not allow the damage location to be determined. However, in the closed-loop plots the impact of damage is more statistically significant, showing that not only is the stiffness matrix clearly changed, but that it is most likely k_3 that is changed. The test statistic for K_{11} is small, indicating no significant difference in mean values, for both the open-loop and closed-loop cases, as expected, because damage in k_3 does not affect K_{11}. The test statistic for K_{22} and K_{33} is substantially larger for closed-loop SMA than for the open-loop case, indicating that the means are significantly different.

The output feedback results, shown in Fig. 2, are not quite as distinct as in the full-state feedback case, but it is still clear that the sensitivity-enhanced case outperforms the open-loop case. As before, damage is only discernable in the third diagonal element for the open-loop plots, whereas, in the closed-loop data, all three diagonal elements are significantly changed, which makes the presence of damage more easily determined, but still does not permit damage localization.

The output feedback approach is applicable to more complex systems; however, ability to determine the location of the damage will depend heavily on the number and location of sensors.

IV. Conclusions

SMA greatly enhances the shifts in the effective stiffness matrix caused by a small change in the actual stiffness of an individual spring. It has also been shown that the position output feedback case performs nearly as well as the full-state feedback case. SMA provides a means for designing sensitivity enhancing controllers for use in the identification of stiffness damage in simple structures.

Acknowledgments

This research is supported by the National Science Foundation under Grant CMS-9988414 and by NASA under NGT5-40088. The authors are grateful for the support.

References

[1]Ray, L. R., and Tian, L., "Damage Detection in Smart Structures Through Sensitivity Enhancing Feedback Control," *Journal of Sound and Vibration*, Vol. 227, No. 5, 1999, pp. 987–1002.

[2]Ray, L. R., Koh, B.-H., and Tian, L., "Damage Detection and Vibration Control in Smart Plates: Towards Multifunctional Smart Structures," *Journal of Intelligent Material Systems and Structures*, Vol. 11, No. 9, 2000, pp. 657–739.

[3]Solbeck, J. A., Koh, B.-H., and Ray, L. R., "A Comparison of Damage Detection Methodologies Using Analytic Models and Identified Models," *Proceedings of the 43rd AIAA/ASME/ASCE/AHS/ASC Structures, Structural Dynamics, and Materials Conference*, Vol. 4, AIAA, Reston, VA, 2002, pp. 2717–2727.

[4]Phan, M. Q., Horta, L. G., Juang, J.-N., and Longman, R. W., "Linear System Identification via an Asymptotically Stable Observer," *Journal of Optimization Theory and Applications*, Vol. 79, No. 1, 1993, pp. 59–86.

[5]Alvin, K. F., and Park, K. C., "Second-Order Structural Identification Procedure via State-Space-Based System Identification," *AIAA Journal*, Vol. 32, No. 2, 1994, pp. 397–406.

[6]Nalitolela, N. G., Penny, J. E. T., and Friswell, M. I., "Mass or Stiffness Addition Technique for Structural Parameter Updating," *International Journal of Analytical and Experimental Modal Analysis*, Vol. 7, No. 3, 1992, pp. 157–168.

[7]Cha, P. D., and Gu, W., "Model Updating Using an Incomplete Set of Experimental Modes," *Journal of Sound and Vibration*, Vol. 233, No. 4, 2000, pp. 587–600.

[8]Lew, J.-S., and Juang, J.-N., "Structural Damage Detection Using Virtual Passive Controllers," *Journal of Guidance, Control, and Dynamics*, Vol. 25, No. 3, 2002, pp. 419–424.

[9]Juang, J.-N., and Pappas, R. S., "An Eigensystem Realization Algorithm for Model Parameter Identification and Model Reduction," *Journal of Guidance, Control, and Dynamics*, Vol. 8, No. 5, 1985, pp. 620–627.

A. Chattopadhyay
Associate Editor

Thermal Postbuckling of Uniform Spring-Hinged Columns Using a Simple Method

G. Venkateswara Rao* and K. Kanaka Raju†
Vikram Sarabhai Space Center, Trivandrum 695 022, India

Nomenclature

A	=	area of cross section
a	=	lateral displacement at the middle of the column
c	=	as defined in Eq. (41)
E	=	Young's modulus
I	=	area moment of inertia
k_1, k_2	=	stiffnesses of the rotational spring (Fig. 1)
L	=	length of the column
P	=	axial compressive load
P_{cr}	=	critical load
P_{NL}	=	postbuckling load
r	=	radius of gyration
T	=	temperature
T_a	=	axial tension developed as a result of large deformations
T_{cr}	=	critical temperature
U	=	strain energy
u	=	axial displacement
W	=	work done by the load P
w	=	lateral displacement
x	=	axial coordinate
α	=	coefficient of linear thermal expansion
β_1, β_2	=	coefficients in Eq. (4)
γ_1, γ_2	=	rotational spring stiffness parameters, $(k_1 L/EI, k_2 L/EI)$
λ	=	load parameter, (PL^2/EI)
λ_{cr}	=	critical load parameter, $(P_{cr}L^2/EI)$
λ_{NL}	=	postbuckling load parameter, $(P_{NL}L^2/EI)$
λ_{Ta}	=	axial tension parameter, $(T_a L^2/EI)$

Superscript

$()'$	=	differentiation with respect to x

Introduction

In a recent Note,[1] the authors have proposed a simple intuitive method to predict the thermal postbuckling behavior of uniform columns, with axially immovable ends, with classical boundary conditions like pinned or clamped at the ends. This method, basically, requires the linear thermal buckling load and the tension developed in the column caused by large deformations.

In actual practice, the classical boundary condition like pinned and clamped are difficult to realize, and the end conditions will be somewhere in between the pinned and clamped ones. This situation can be simply represented by applying elastic rotational springs with a specified stiffness and making the lateral displacements at the ends zero. The limiting cases of pinned and clamped conditions can be obtained by making the rotational spring stiffness either zero or very large.

Received 5 February 2003; revision received 1 August 2003; accepted for publication 1 September 2003.

*Group Director, Structural Engineering Group; gv_rao@vssc.org.

†Head, Computational Structural Technology Division, Structural Engineering Group.